Macromolecular Materials and Engineering
www.mme-journal.de

Large-Scale Preparation of Polymer Nanocarriers by High-Pressure Microfluidization

Mohammad Shafee Alkanawati, Frederik R. Wurm, Héloïse Thérien-Aubin, and Katharina Landfester**

Polymer nanocarriers are used as transport modules in the design of the next generation of drug delivery technology. However, the applicability of nanocarrier-based technology depends strongly on our ability to precisely control and reproduce their synthesis on a large scale because their properties and performances are strongly dependent on their size and shape. Fundamental studies and practical applications of polymer nanocarriers are hampered by the difficulty of using the current methods to produce monodispersed nanocarriers in large quantities and with high reproducibility. Here, a versatile and scalable approach is reported for the large-scale synthesis of polymer nanocarriers from water-in-oil miniemulsions. This method uses microfluidization to perform a controlled emulsification and is proven to be effective to prepare nanocarriers of different biopolymers (polysaccharides, lignin, proteins) up to 43 g min^{-1} with reproducible size and distribution.

1. Introduction

Nanocarriers, colloids used as transport modules, have been gaining scientific and industrial importance over the past decades.[1] They are being used in a variety of applications, from the biomedical[2–4] to the agricultural fields.[5–7] Nanocarriers are used to deliver payloads and can target specific cells and organs,[8] while improving the bioavailability, stability,[9] and efficiency of the payloads.[10]

Many factors influence the performances of a nanocarrier in a bioenvironment. The behavior of a nanocarrier is not only affected by its chemical composition and functionalization, but also its size and shape will also affect bioavailability, biodistribution, kinetic of release, and cellular uptake.[11] Polymer nanocarriers have imposed themselves as front-runners in the development of new technologies due to their versatility in terms of composition, functionalization, and size control.[12] Polymer nanocarriers can be prepared by a variety of methods whether it is by the dispersion of premade polymers or by the dispersion of polymer precursors. Polymer nanocarriers prepared from monomers are usually synthesized by dispersion, suspension emulsion, or miniemulsion polymerization, while the preparation of polymer nanocarriers made from preformed polymers usually occurs by coacervation methods such as salting out,[13] emulsification–diffusion,[14] nanoprecipitation, and supercritical fluid technology.[15,16] Among those different preparation techniques, miniemulsion is particularly attractive due to its ability to prepare nanocarriers from either monomer or polymer while allowing for the efficient loading of large doses of therapeutic agents, which can be lipophilic and/or hydrophilic compounds.[17] Furthermore, miniemulsion provides the opportunity to finely tune particle size distribution while preparing emulsion with high solid content of polymers.[18–20]

The crosslinking of polymer-containing nanodroplets formed by miniemulsion is a particularly attractive method to produce nanocarriers (**Figure 1**). Hollow nanocapsules can be prepared by a polyaddition or polycondensation reaction occurring at the droplets interface.[21] In order to prepare nanocarriers, the polymer is dissolved in a good solvent and emulsified with an immiscible nonsolvent forming the continuous phase. After the emulsification, a crosslinking agent, soluble in the continuous phase, is added to the emulsion and the polyaddition or polycondensation reaction between the polymer and crosslinking agent occurs at the surface of the droplet. When the reaction kinetic is fast enough, a shell insoluble in both phases can be formed at the interface.[22]

To control the size and size distribution of the nanocapsules prepared by the polyaddition/polycondensation reaction at the droplet interface, it is critical to control the preparation of the miniemulsion used as a precursor. The two main factors leading to the broadening of the size distribution of the nanodroplets during miniemulsion are (i) Ostwald ripening and (ii) coalescence of the droplets occurring through collision. The coalescence could be controlled by the addition of an appropriate surfactant, which provides electrostatic or steric stabilization thus preventing droplet coalescence. Ostwald ripening is affected by multiple factors such as droplet size, Laplace pressure, polydispersity, and solubility of the dispersed phase in the continuous phase. In general, Ostwald ripening could be limited by the addition of compounds increasing the osmotic pressure in the system. These chemicals need to be highly insoluble in the continuous phase but completely soluble in the

M. S. Alkanawati, Dr. F. R. Wurm, Dr. H. Thérien-Aubin, Prof. K. Landfester
Max Planck Institute for Polymer Research, Mainz, Germany
E-mail: therien@mpip-mainz.mpg.de; landfest@mpip-mainz.mpg.de
The ORCID identification number(s) for the author(s) of this article can be found under https://doi.org/10.1002/mame.201700505.

DOI: 10.1002/mame.201700505

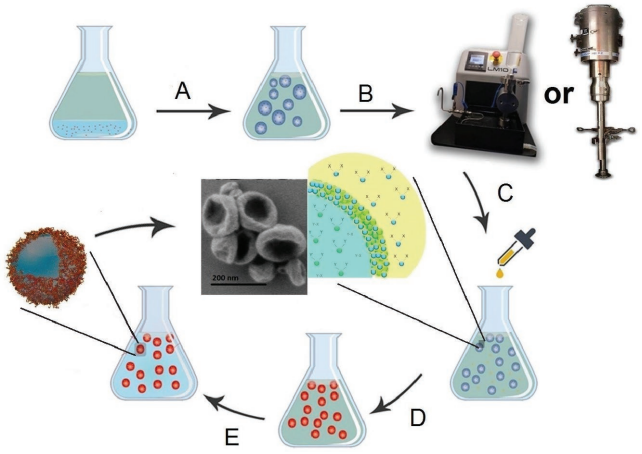

Figure 1. Synthesis of nanocarriers by polyaddition/polycondensation at the droplet interface in miniemulsion. A) Preparation of the inverse preemulsion, B) preparation of the inverse miniemulsion by ultrasonication or microfluidization, C) addition of the crosslinking agent, D) polyaddition/polycondensation at the droplets interface, and E) transfer to water.

dispersed phase, resulting in an increase of the osmotic pressure from the outside to the inside of the droplet and leading to an increased stability of the droplets.[23]

Typically, miniemulsions are prepared by making a coarse preemulsion by simple stirring followed by ultrasonication in order to break down the large and dispersed droplets of the preemulsion into a final well-controlled miniemulsion.[19] The ultrasound waves are converted in the shear forces required to break down the large droplets. Alternative techniques might be used to break down the preemulsion such as rotor–stator dispersion with special rotor geometries, high-pressure homogenization, and microfluidization.[19]

The ultrasound waves are converted to energy by cavitation in the entire sample; the ultrasound waves form bubbles in the liquid, those bubbles are implosive, and during their collapse energy is produced leading to the reduction in the size of the droplets in the miniemulsion.[19,24] In order to generate sufficient energy to break down the preemulsified droplets, the ultrasounds need to be applied to the system for a long duration. The unevenly distributed events of cavitation-induced droplet disruption and the long duration of ultrasound application lead to an inherent size distribution of the droplets formed during miniemulsion.

Due to the limitation of the ultrasonication step—mainly production of limited quantities and a poor batch-to-batch reproducibility—it is critical to develop alternative methods to scale-up the preparation of nanocapsules by miniemulsion.[25] Here we used microfluidization to produce the precursor droplets used in the preparation of polymer nanocapsules. During microfluidization, a large pressure produces a flow of the preemulsified mixture at high velocity through an interaction chamber. This interaction chamber consists of microchannels having diameters in the range of 50 and 200 µm. The flow is divided into separated microstreams by the microchannels inside the chamber. The microstreams are brought together in an impinging geometry creating high impact energy and shear stresses on the droplets. Consequently, a high mechanical stress is applied on the droplet in a localized area for a very short time; this produces a well-controlled emulsion.[26] Furthermore, the size and size distribution of the resulting nanocapsules can be controlled by tuning the processing conditions. We compared the efficiency of microfluidization to state-of-the-art technology used in the preparation of polymer nanocapsules and demonstrate the versatility of this approach. This versatility of the microfluidization preparation process was also demonstrated by employing different biopolymers: polysaccharides, proteins, or lignin were used as models for enzymatically degradable drug carriers and the scaling up of their preparation procedure.

2. Experimental Section

2.1. Materials

All chemicals and materials were used as received if not otherwise mentioned. Bovine serum albumin, adipic acid dihydrazide, 2,4-toluene diisocyanate (TDI), sulforhodamine 101 (SR 101), lignin sulfuric acid sodium salt (# 471038), and phenyl dichlorophosphate were purchased from Sigma Aldrich. Cyclohexane was purchased from VWR Chemicals. A 10 wt% aqueous solution of hydroxyethyl starch (HES) was purchased from Fresenius Kabi. Sodium dodecyl sulfate was purchased from Alfa Aesar. Polyglycerol polyricinoleate (PGPR) was provided from Danisco and was purified first by dissolution in hexane followed by centrifugation (2000 rpm) to precipitate solid particles, then the supernatant was recover and the purified PGPR was dried by rotary evaporation.

2.2. Instrumentation

The miniemulsions were prepared with a microfluidizer LM10 (Microfluidics corporation) or Sonifier W-450 D (Branson Ultrasonics). The size of the particles was measured by dynamic light scattering (DLS) at 25 °C using a Nicomp 380 (Particle Sizing Systems). A centrifuge 3-30KHS (Sigma Centrifuges) was used at 5000 rpm to recover the nanocarriers. Morphological investigations were performed by scanning electron microscopy (SEM) LEO Gemini 1530; the samples were prepared by placing 20 µL of diluted nanocolloid suspension onto a 300-mesh carbon-coated copper grid and dry under ambient conditions. Infrared spectroscopy (FT-IR) was performed on a spectrum BX (Perkin Elmer). Surface tension was measured by DCAT 21 (Dataphysics). The dynamic viscosity was measured with an Ubbelohde viscosimeter using an AVS370 setup (SCHOTT). The kinematic viscosity was calculated from dynamic viscosity taking into account the density determined with a densimeter DM40 (Mettler Toledo).

2.3. Synthesis of Nanocarriers

Unless noted otherwise, the nanocarriers were prepared following the recipe below. The aqueous phase was prepared by dissolving 160 mg of NaCl in 10.2 g or a 10 wt% solution of polymer. The continuous phase (oil phase) was prepared by

dissolving 1 g of PGPR in 60 g of cyclohexane. The oil phase was added dropwise to the stirred aqueous phase to form the inverse preemulsion. The preemulsified system was then emulsified by either ultrasound (pulsed program (1 s on, 1 s off) for 3 min at 70% amplitude) or by two cycles through the microfluidizer (69 MPa). A solution of 1 g of crosslinking agent and 660 mg of PGPR in 40 g cyclohexane was then added dropwise to the miniemulsion. The suspension was stirred for 24 h at room temperature until the crosslinking reaction was complete. The resulting nanocarriers were purified by two cycles of centrifugation to remove unreacted crosslinkers and excess of surfactant.

3. Results and Discussion

In order to optimize the preparation of polymer nanocarriers, nanocapsules made of HES crosslinked with TDI were chosen as model system. HES nanocapsules have been previously prepared by polyaddition at the droplet interface in reverse miniemulsion,[27] and used as nanocarriers for parenteral drug delivery.[28] The first step in the formation of HES nanocarriers is the preparation of a stable miniemulsion of an aqueous solution of HES (10 wt%) in cyclohexane containing PGPR. PGPR is a polymeric hydrophilic emulsifier with an hydrophilic-lipophilic balance (HLB) value of 1.5 ± 0.5 and was used here to stabilize the miniemulsion by preventing the coalescence of the nanodroplets through steric repulsion.[29] The quality of the nanocapsules prepared was evaluated by DLS. The quality was defined by three parameters: the average diameter ($\overline{D}$) of the swollen nanocapsule, the broadness of the size distribution and the reproducibility or batch-to-batch variation (R) defined as

$$R = \sqrt{\frac{\sum_{i=1}^{N}\left(D_i - \overline{D}\right)^2}{N-1}} \quad (1)$$

where D_i is the average diameter of a given batch and N the number of batches ($N > 3$). Finally, the broadness of the size distribution was defined by its polydispersity index PDI

$$\mathrm{PDI} = \left(\frac{\sigma_i}{D_i}\right)^2 \quad (2)$$

where σ_i is the standard deviation of the size distribution.

3.1. Optimization of Microfluidization Process

To prepare homogenous and well-controlled miniemulsions, a variety of factors can be tuned to influence the quality and size of the final nanocarriers. This can be achieved by varying either the operating pressure or the duration during which the pressure is applied (i.e. the number of time the emulsion is cycled through the microfluidizer). The coalescence of the nanodroplets formed during miniemulsification could be delayed and prevented by using a sufficient amount of surfactant. **Figure 2**A shows the size and size distribution of HES nanocapsules prepared using an oil phase containing an increasing amount (0.5–4 wt%) of PGPR. The critical amount of surfactant needed to stabilize

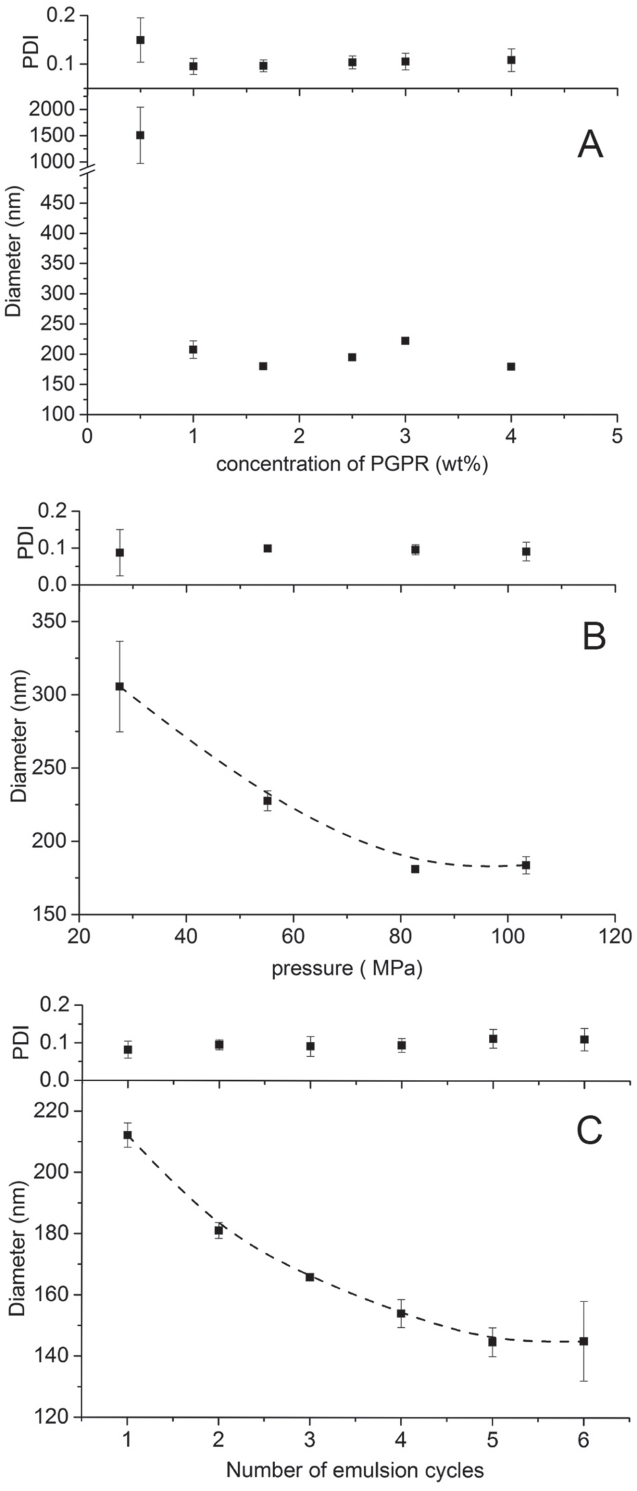

Figure 2. Effect of processing parameter during emulsification by microfluidization on the final particle size and polydispersity of HES nanocarriers. A) Concentration of surfactant in the oil phase. B) Operating pressure. C) Number of emulsion cycles.

the HES droplets was determined to be 1 wt% of PGPR. When the PGPR was present in a concentration above 1 wt%, the nanocapsule size and size distribution were similar in every

case, indicating that a sufficient amount of surfactant was present to stabilize the new interface created during the microfluidization (as measured at 69 MPa). However, at a concentration of PGPR of 0.5 wt% or lower, aggregation was observed. The concentration of PGPR played a significant role in the formation of homogeneous nanodroplets and thus homogeneous nanocolloids.

The size of the nanodroplets formed during miniemulsification strongly depends on the energy given to the system to break down the preemulsion.[19] During microfluidization, this can be controlled through two parameters, the pressure used to propel the stream of preemulsion in the interaction chamber and the number of time the emulsion is passed through the interaction chamber. Figure 2B shows the effect of the operating pressure on the size and size distribution of the HES nanocapsules. The results show that increasing the pressure from 27.6 to 103 MPa led to a reduction in size of 40% with no significant change in the sample polydispersity. By increasing the pressure in the microfluidizer, the velocity of the fluid inside the microchannel was increased from 250 to 600 mL min^{-1} when the pressure was increased from 27.6 to 103 MPa. In the microfluidizer, the pressure applied is transformed into shear and impact forces. These disruptive forces play a key role in overcoming both the surface energy and the viscoelastic energy of the droplet resulting in a smaller average particle size after a cycle through the microfluidizer.

An alternative way to increase the energy given to break down the preemulsion into a well-controlled miniemulsion is to pass the emulsified suspension multiple times through the microfluidizer. Figure 2C shows the effect of increasing the number of passes through the microfluidizer on the size and size distribution of the HES nanocapsules formed. Narrow and homogeneous particle size distributions were obtained already after two and three emulsion cycles.

During the preparation of a miniemulsion, the total force applied to the system will influence the final droplet size. Generally, increasing the microfluidization pressure and the number of cycles should result in a decrease in droplets size. However, in the present case, above 69 MPa or after more than three cycles through microfluidizer, no significant decrease in nanodroplet size was observed, while both the polydispersity index and the batch-to-batch variability increased. This phenomenon is referred to as overprocessing.[30] It could be partially attributed to the efficiency of the emulsifier (the speed at which the surfactant molecules absorbed on the newly created surfaces), and to an increase in the Brownian motion, increasing the probability of collision leading to coalescence at higher energy input. During overprocessing, two opposite processes compete. On one side, the formation of new droplets by breaking down the existing lager droplets and, on the other side, the droplet–droplet coalescence. Once new droplets are formed by breaking down an initial and bigger droplet, new interfaces are created and the surfactant molecules need to adsorb onto these fresh interfaces. If the timescale of collision is shorter than the timescale of adsorption, the fresh interfaces of the newly formed droplets will not be fully covered by surfactant molecules and those interfaces will not be fully stabilized, leading to an increased droplet–droplet coalescence evidenced by a broader size distribution.[31]

3.2. Comparison between Microfluidization and Ultrasonication in the Preparation of HES Nanocarriers

The current state-of-the-art method for the preparation of nanocarriers by the miniemulsion process relies on the use of ultrasound as a source of disruptive forces. Preparation of HES nanocarriers was realized using either ultrasonication or microfluidization (**Figure 3**) and the resulting nanocapsules were compared in terms of particle size and size distribution as well as batch-to-batch variability. The results obtained are summarized in **Table 1**. The average size of the nanocapsules formed was smaller by microfluidization. This was only related to the fact that the energy provided to the system was marginally higher during microfluidization than during ultrasonication. More interestingly, both the size distribution (PDI) and the batch-to-batch variability decreased when using microfluidization in comparison to ultrasonication. The narrow size distribution observed after microfluidization could be explained by the fact that the energy provided during microfluidization is more homogeneous compared to the energy produced by the cavitation-induced ultrasounds. Furthermore, the reduced batch-to-batch variability observed with the use of the microfluidizer could be ascribed to the precise control over the experimental conditions when compared to ultrasonication.

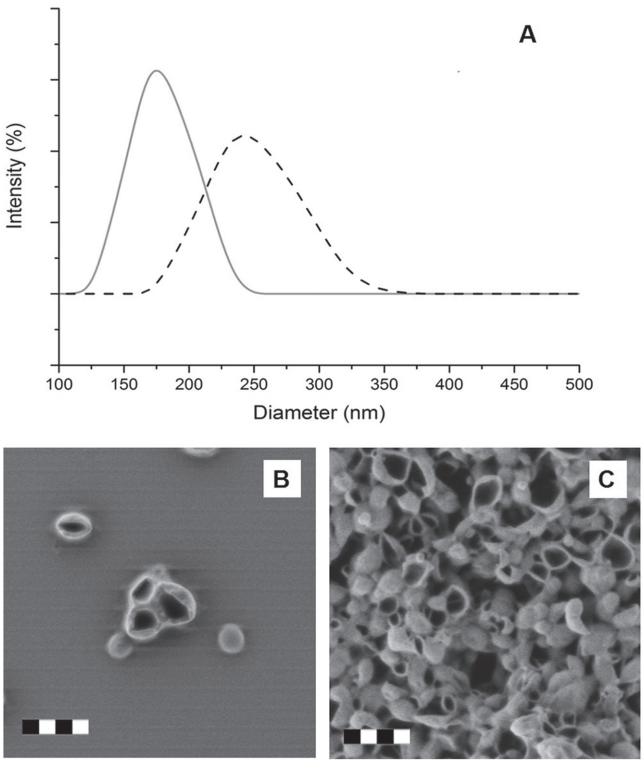

Figure 3. A) Particle size distribution of HES nanocarriers prepared by microfluidization (solid line) and by ultrasonication (dashed line). B) SEM image of HES nanocarriers prepared by microfluidization. C) SEM image of HES nanocarriers prepared by ultrasonication. The scale bars are 400 nm.

Table 1. Comparison between HES nanocapsules prepared by microfluidization and ultrasonication.

	Microfluidizer	Ultrasound
Production	430 g/10 min	150 mg/10 min
Average size [nm]	185	230
Batch-to-batch variation [nm]	9	27
Average PDI	0.05	0.09

3.3. Versatility of the Method

To demonstrate the universality of using microfluidization in the production of nanocapsules, alternative precursors and crosslinking chemistries were used (see the Supporting Information).

In the first case, the polysaccharide HES was substituted by the well-defined protein bovine serum albumin and the very ill-defined, aromatic lignin, while the same crosslinking agent (TDI), operating pressure, and surfactant concentration were used. These biopolymers were chosen in order to generate nanocarriers that might be used in drug delivery for vertebrates (HES, albumin) or plants (lignin), depending on the enzymes, present in the respective organisms. **Figure 4** shows the SEM images and particle size distributions of the HES, albumin, and lignin nanocarriers obtained. In every case, high-quality nanocarriers were obtained (PDI < 0.08). All the nanocarriers whether made of lignin, albumin, or HES prepared by microfluidization have smaller size and better size distribution than those that prepared by ultrasonication.[2,32] However, Figure 4 clearly shows that the nanocarriers produced with albumin (160 ± 5 nm) and lignin (166 ± 4 nm) were smaller than those made of HES (180 ± 3 nm). The variation in nanocapsule size can be related to the size of the nanodroplets generated during microfluidization. The droplet size of the miniemulsion strongly depends on the droplet internal viscosity.[33,34] The dynamic viscosity of the albumin, lignin, and HES aqueous solution used as the dispersed phase used in the preparation of the nanocarriers was, respectively, 1.51, 1.58, and 1.84 cP. An increase in the internal viscosity of the dispersed phase would lead to an increase in droplet size when the same energy is applied to the system to generate the emulsion. During the miniemulsion step, the droplets are only broken into smaller nanodroplets when the energy provided to the system by the microfluidizer exceeds contributions of interfacial energy of the precursor droplets and their viscoelastic energy. As the viscosity of the dispersed phase increases, the viscoelastic energy increases and the reduction in the average size of the droplet during microfluidization is impeded leading to the formation of larger precursor droplets and larger nanocapsules after crosslinking.[33,34]

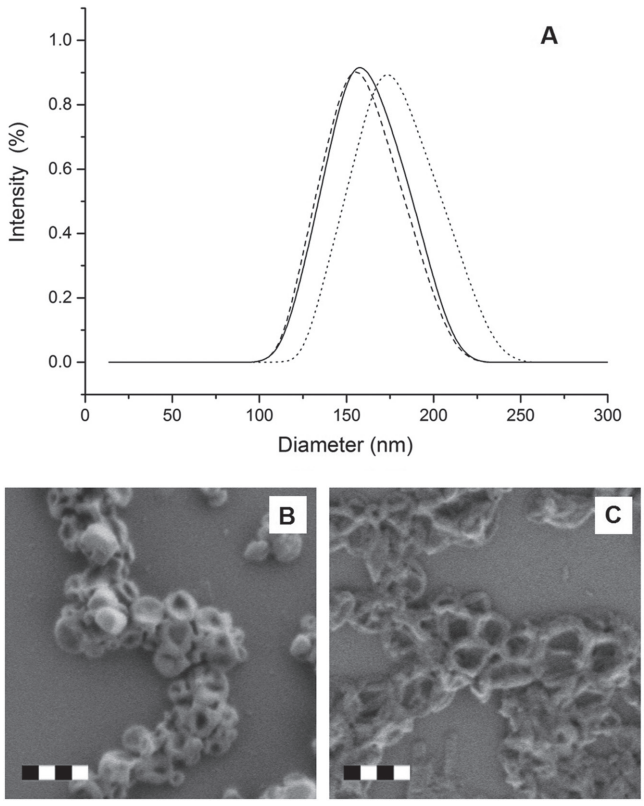

Figure 4. A) Particle size distribution of biopolymer nanocarriers prepared by microfluidization for lignin (solid line), HES (dotted line), and albumin (dashed line). B) SEM image of albumin nanocarriers. C) SEM image of lignin nanocarriers. Scale bars are 400 nm.

To further demonstrate the generality and compatibility of the microfluidizer process with a variety of chemical compounds and conditions, the crosslinking mechanism leading to the formation of the nanocarrier shell was modified. HES nanocarriers were prepared using either TDI as described previously or other potentially degradable linkages: phenyl dichlorophosphate was used for the direct crosslinking of the OH-groups present in HES, in a manner similar to the previously reported interfacial polycondensation of bisphenol-A with phosphoric acid chloride.[35] Alternatively, HES modified with aldehyde groups was crosslinked with adipic acid dihydrazide to form a crosslinked hydrazone network (Supporting Information). **Figure 5** shows the SEM images and the particle size distributions obtained for those various HES nanocarriers.

DLS was used to measure the particles size distributions; the average size of HES crosslinked with TDI was smaller than the average size obtained for nanocapsules obtained after the crosslinking of HES with phenyl dichlorophosphate (185 ± 10 and 230 ± 25 nm, respectively). However, the size of the dry nanocapsules measured from the SEM images was similar (100 ± 30 nm for TDI and 100 ± 20 nm for phenyl dichlorophosphate). The difference in dry and hydrated diameter could be ascribed to differences in crosslinking densities and hydrophilicity between the HES nanocapsules prepared after crosslinking with TDI and phenyl dichlorophosphate. The hydrodynamic diameter of the swollen nanocapsules measured by DLS reflected the larger swelling of the HES nanocapsules crosslinked with phenyl dichlorophosphate when compared to the nanocapsules prepared with TDI.

Figure 5 also shows that nanocarriers prepared with HES and adipic acid dihydrazine are smaller than the other HES nanocarriers. The SEM images (Figure 5C) also demonstrate that those nanocarriers are particles rather than capsules. In

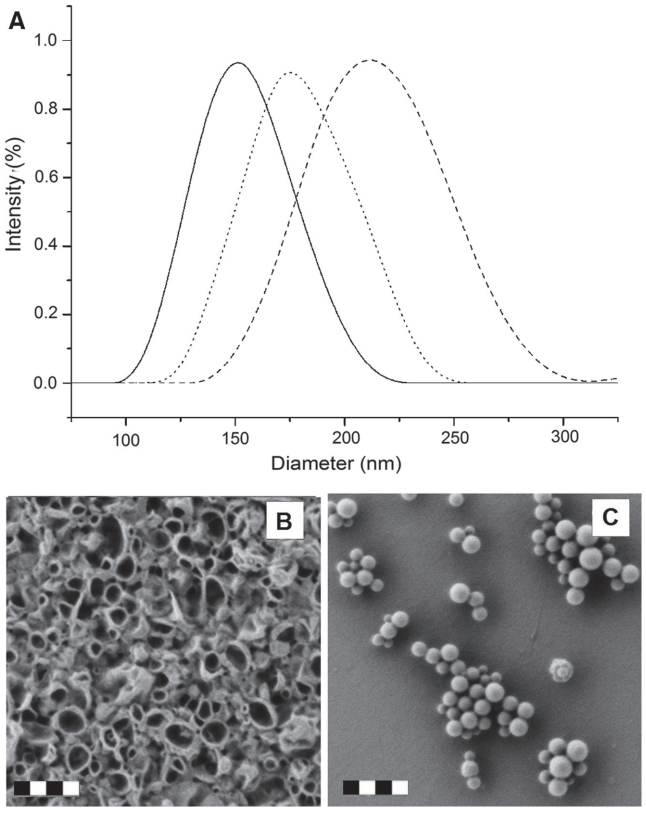

Figure 5. A) Particle size distribution of HES nanocarriers with after crosslinking with phenyl dichlorophosphate (solid line), TDI (dotted line), and adipic acid dihydrazide (dashed line). B) SEM image of HES nanocarriers crosslinked with phenyl dichlorophosphate. C) SEM image of HES nanocarriers crosslinked with adipic acid dihydrazide. Scale bars are 400 nm.

comparison to TDI or phenyl dichlorophosphate, adipic acid dihydrazide is more water soluble. Due to the insolubility of TDI and phenyl dichlorophosphate in water, the crosslinking reaction was only occurring at the interface of the aqueous droplet of HES solution leading to the formation of the outer shell of the nanocapsule. However, in the case of adipic acid dihydrazide, the solubility of the crosslinker in the dispersed phase allowed for the diffusion of the crosslinker inside the HES droplet leading to the formation of nanoparticles rather than nanocapsules. The resulting extensive crosslinking was also responsible for the decrease in the nanocolloid average diameter observed between the HES particles obtained after crosslinking with adipic acid dihydrazide in comparison to the capsules formed after the crosslinking of HES with TDI or phenyl dichlorophosphate.

4. Conclusions

Nanocarriers have been prepared on a large scale (43 g min^{-1}) by using a microfluidizer to generate the precursor nanodroplets. The use of microfluidization allowed us to overcome inherent problems typically associated with the scaling up of the preparation of nanocapsules, i.e., increase in reaction volume (larger PDI) or numbering-up (larger batch-to-batch variability). We were able to produce nanocapsules of higher quality (low PDI and batch variability) and a 300-fold increase in the production output was observed. The size and size distribution of the nanocarrier produced was easily tuned by the variation of the operating conditions. To demonstrate the versatility of the technique, different precursor building blocks of the nanocapsules were used: polysaccharide, protein, and functional molecules and used in presence of different crosslinking chemistries. These results, coupling with the fact that microfluidization could be implemented in-line, paves the way to the production of nanocapsules for drug delivery on an industrial scale.

Supporting Information

Supporting Information is available from the Wiley Online Library or from the author.

Acknowledgements

This project received funding from the Biobased Industries joint undertaking under the European Union's Horizon 2020 research and innovation program under grant agreement 720708. The authors gratefully acknowledge the financial support of Deutsche Forschungsgemeinschaft (DFG Sonderforschungsbereich SFB 1066). H.T.-A. acknowledges the Alexander von Humboldt stiftung for financial support.

Conflict of Interest

The authors declare no conflict of interest.

Keywords

microfluidization, miniemulsion, nanocarriers

Received: October 9, 2017
Revised: November 9, 2017
Published online: December 14, 2017

[1] S. Ganta, H. Devalapally, A. Shahiwala, M. Amiji, *J. Controlled Release* **2008**, *126*, 187.
[2] D. Yiamsawas, G. Baier, E. Thines, K. Landfester, F. R. Wurm, *RSC Adv.* **2014**, *4*, 11661.
[3] R. Karim, C. Palazzo, B. Evrard, G. Piel, *J. Controlled Release* **2016**, *227*, 23.
[4] N. Chen, L. A. Dempere, Z. Tong, *ACS Sustainable Chem. Eng.* **2016**, *4*, 5204.
[5] A. Gogos, K. Knauer, T. D. Bucheli, *J. Agric. Food Chem.* **2012**, *60*, 9781.
[6] J. S. Duhan, R. Kumar, N. Kumar, P. Kaur, K. Nehra, S. Duhan, *Biotechnol. Rep.* **2017**, *15*, 11.
[7] A. Goswami, I. Roy, S. Sengupta, N. Debnath, *Thin Solid Films* **2010**, *519*, 1252.
[8] F. Danhier, O. Feron, V. Préat, *J. Controlled Release* **2010**, *148*, 135.
[9] V. Bali, M. Ali, J. Ali, *Int. J. Pharm.* **2011**, *403*, 46.

[10] L. S. Jabr-Milane, L. E. van Vlerken, S. Yadav, M. M. Amiji, *Cancer Treat. Rev.* **2008**, *34*, 592.
[11] A. Albanese, P. S. Tang, W. C. W. Chan, *Annu. Rev. Biomed. Eng.* **2012**, *14*, 1.
[12] J. P. Rao, K. E. Geckeler, *Prog. Polym. Sci.* **2011**, *36*, 887.
[13] R. H. Gaonkar, S. Ganguly, S. Dewanjee, S. Sinha, A. Gupta, S. Ganguly, D. Chattopadhyay, M. Chatterjee Debnath, *Sci. Rep.* **2017**, *7*, 530.
[14] H.-Y. Kwon, J.-Y. Lee, S.-W. Choi, Y. Jang, J.-H. Kim, *Colloids Surf., A* **2001**, *182*, 123.
[15] Z. Zhang, D. W. Grijpma, J. Feijen, *J. Controlled Release* **2006**, *111*, 263.
[16] B.-Q. Chen, R. K. Kankala, A.-Z. Chen, D.-Z. Yang, X.-X. Cheng, N.-N. Jiang, K. Zhu, S.-B. Wang, *Int. J. Nanomed.* **2017**, *12*, 1877.
[17] S.-H. Hu, S.-Y. Chen, X. Gao, *ACS Nano* **2012**, *6*, 2558.
[18] T. Nagaoka, T. Fukuda, S. Yoshida, H. Nishimura, D. Yu, S. Kuroda, K. Tanizawa, A. Kondo, M. Ueda, H. Yamada, H. Tada, M. Seno, *J. Controlled Release* **2007**, *118*, 348.
[19] K. Landfester, in *Colloid Chemistry II* (Ed: M. Antonietti), Springer, Berlin **2003**, pp. 75–123.
[20] M. Wu, E. Rotureau, E. Marie, E. Dellacherie, A. Durand, in *Emulsion Science and Technology*, (Ed: T. Tadros), Wiley-VCH, Weinheim **2009**, pp. 107–132.
[21] K. Piradashvili, E. M. Alexandrino, F. R. Wurm, K. Landfester, *Chem. Rev.* **2016**, *116*, 2141.
[22] Q. Zhang, Y. Shi, X. Zhan, F. Chen, *Colloids Surf., A* **2012**, *393*, 17.
[23] K. Landfester, *Top. Curr. Chem.* **2003**, *227*, 75.
[24] S. M. Jafari, Y. He, B. Bhandari, *J. Food Eng.* **2007**, *82*, 478.
[25] J. M. Asua, *Prog. Polym. Sci.* **2014**, *39*, 1797.
[26] S. L. Anna, N. Bontoux, H. A. Stone, *Appl. Phys. Lett.* **2003**, *82*, 364.
[27] B. Kang, P. Okwieka, S. Schöttler, S. Winzen, J. Langhanki, K. Mohr, T. Opatz, V. Mailänder, K. Landfester, F. R. Wurm, *Angew. Chem., Int. Ed.* **2015**, *54*, 7436.
[28] D. Narayanan, S. Nair, D. Menon, *Int. J. Biol. Macromol.* **2015**, *74*, 575.
[29] R. Wilson, B. J. van Schie, D. Howes, *Food Chem. Toxicol.* **1998**, *36*, 711.
[30] A. Desrumaux, J. Marcand, *Int. J. Food Sci. Technol.* **2002**, *37*, 263.
[31] S. Mahdi Jafari, Y. He, B. Bhandari, *Int. J. Food Prop.* **2006**, *9*, 475.
[32] K. Piradashvili, M. Fichter, K. Mohr, S. Gehring, F. R. Wurm, K. Landfester, *Biomacromolecules* **2015**, *16*, 815.
[33] A. Gupta, V. Narsimhan, T. A. Hatton, P. S. Doyle, *Langmuir* **2016**, *32*, 11551.
[34] A. Gupta, H. B. Eral, T. A. Hatton, P. S. Doyle, *Soft Matter* **2016**, *12*, 1452.
[35] E. M. Alexandrino, M. Wagner, K. Landfester, F. R. Wurm, *Macromol. Chem. Phys.* **2016**, *217*, 1941.

